Dalton Transactions

Accepted Manuscript

ROYAL SOCIETY OF CHEMISTRY

www.rsc.org/dalton

Journal Name

RSCPublishing

ARTICLE

Charge transfer complexes of fullerenes containing $C_{60}^{\bullet-}$ and $C_{70}^{\bullet-}$ radical anions with paramagnetic $Co^{II}(dppe)_2Cl^+$ cations (dppe: 1,2-bis(diphenylphosphino)ethane)

Cite this: DOI: 10.1039/x0xx00000x

Received 00th January 2012,
Accepted 00th January 2012

DOI: 10.1039/x0xx00000x

www.rsc.org/

Dmitri V. Konarev,*[a] Sergey I. Troyanov,[b] Akihiro Otsuka,[c] Hideki Yamochi,[c] Gunzi Saito[d,e] and Rimma N. Lyubovskaya[a]

The reduction of $Co^{II}(dppe)Cl_2$ with sodium fluorenone ketyl produces red solution containing the Co^I species. The dissolution of C_{60} in the obtained solution followed by the precipitation of crystals by hexane yields salt $\{Co^I(dppe)_2^+\}(C_{60}^{\bullet-})\cdot 2C_6H_4Cl_2$ and novel complex $\{Co(dppe)_2Cl\}(C_{60})$ (**1**). With C_{70}, only the crystals of $\{Co(dppe)_2Cl\}(C_{70})\cdot 0.5C_6H_4Cl_2$ (**2**) are formed. Complex **1** contains zig-zag fullerene chains whereas closely packed double chains are formed from fullerenes in **2**. According to optical spectra and magnetic data charge transfer occurs in both **1** and **2** with the formation of the $Co^{II}(dppe)_2Cl^+$ cations and the $C_{60}^{\bullet-}$ or $C_{70}^{\bullet-}$ radical anions. In spite of close packing in crystals, $C_{60}^{\bullet-}$ or $C_{70}^{\bullet-}$ retain in monomeric form at least down to 100 K. Effective magnetic moments of **1** and **2** of 1.98 and 2.27 μ_B at 300 K, respectively, do not attain the value of 2.45 μ_B expected for the system with two non-interacting S = 1/2 spins at full charge transfer to fullerenes. Most probably diamagnetic $\{Co^I(dppe)_2Cl\}^0$ and neutral fullerenes are partially preserved in the samples which can explain weak magnetic coupling of spins and the absence of fullerene dimerization in both complexes. The EPR spectra of **1** and **2** show asymmetric signals approximated by several lines with g-factors ranging from 2.0009 to 2.3325. These signals originate from exchange interaction between paramagnetic $Co^{II}(dppe)_2Cl^+$ cations and fullerene$^{\bullet-}$ radical anions.

Introduction

Ionic compounds of fullerenes possess promising conducting and magnetic properties.[1-4] Crystalline samples of these compounds are generally prepared using organic or solvated metal cations.[5,6] Metallocenes are strong donor molecules to give the charge-transfer (CT) complexes composed of mono- to tri-anionic fullerenes.[7-10] Also, by employing extra reducing agents such as alkali metals or tetrakis(dimethylamino)ethylene (TDAE), anionic fullerene complexes with organometallic cations are prepared. The latter method provided the complexes with $\{(Ph_3P)_3Au^I\}^+$,[11] $Co^I(dppe)_2^+$ [12] and some positively charged Ph_3P-containing gold clusters[13], for example. The organometallic cations can introduce paramagnetic centers into the ionic fullerene systems.

In our previous works we studied coordination compounds of fullerene C_{60} with cobalt in zero oxidation state containing Ph_3P and diphosphine ligands (including 1,2-bis(diphenylphosphino)ethane, dppe) and in some cases benzonitrile.[15-17] In this work we studied the interaction of fullerenes C_{60} and C_{70} with $Co(dppe)_2Cl$ prepared by the reduction of $Co^{II}(dppe)Cl_2$ with sodium fluorenone ketyl. Crystalline $\{Co(dppe)_2Cl\}(C_{60})$ (**1**) and $\{Co(dppe)_2Cl\}(C_{70})\cdot 0.5C_6H_4Cl_2$ (**2**) compounds were obtained together with previously studied salt $\{Co^I(dppe)_2^+\}(C_{60}^{\bullet-})\cdot 2C_6H_4Cl_2$ [12]. We present crystal structures, optical and magnetic properties of these complexes. Compound **2** is a rare example of ionic fullerene structure containing monomeric $C_{70}^{\bullet-}$ radical anions while they form single-bonded $(C_{70}^-)_2$ dimers[18-20] in most of anion radical salts.

Results and discussion

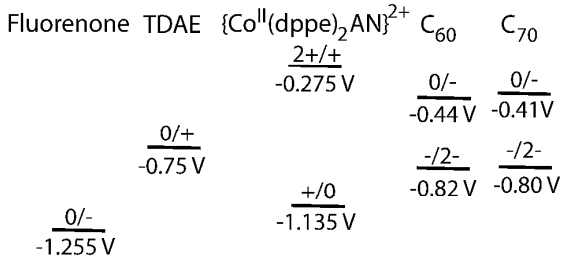

Scheme 1. Redox potentials of the components used in the synthesis of Co(dppe)-fullerene complexes. All potentials are given *vs* SCE.

a). Synthesis

As summarized in Scheme 1, the first reduction potentials for fullerenes C_{60} and C_{70} are -0.44 V and -0.41 V, respectively in dichloromethane *vs* SCE. The second reduction wave is observed at -0.82 and -0.80 V *vs* SCE, respectively in the same solvent.[21] The $\{Co^{II}(dppe)_2(CH_3CN)\}^{2+}$ cations can be reduced electrochemically to $\{Co^{I}(dppe)_2\}^{+}$ at -0.70 V *vs* Fc^+/Fc (-0.275 V *vs* SCE).[22] Previously we used tetrakis(dimethylamino)-ethylene (TDAE) as reductant for $Co^{II}(dppe)Br_2$ and C_{60}.[12] TDAE with the first oxidation potential of $E^{+/0}$ = -0.75 V *vs* SCE[23] generates the Co^{I} species and $C_{60}^{\bullet-}$ in solution which cocrystallize to form the $\{Co^{I}(dppe)_2^{+}\}(C_{60}^{\bullet-})\cdot 2C_6H_4Cl_2$ salt[12]. While $Co^{I}(dppe)_2^{+}$ cation has an odd $S = 1$ or $S = 0$ spin state, only the $C_{60}^{\bullet-}$ signal is observed in the spectrum of this salt. Further reduction of $Co^{I}(dppe)_2^{+}$ to $Co^{0}(dppe)_2$ by TDAE is not possible (Scheme 1) since the conversion takes place at more negative redox potential of -1.56 V *vs* Fc^+/Fc (-1.135 V *vs* SCE)[22]. The $Co^{I}(dppe)_2^{+}$ cation is also too weak a donor to reduce $C_{60}^{\bullet-}$ to C_{60}^{2-}.

Sodium fluorenone ketyl, (fluorenone$^{\bullet-}$)(Na^+) is a stronger reducing agent than TDAE (Scheme 1) with the first oxidation potential of about -1.30 V *vs* Ag/AgCl or (-1.255 V *vs* SCE)[24]. Therefore, this ketyl can also reduce $Co^{II}(dppe)Cl_2$ to generate the Co^{I} species. Potentially it can also reduce $Co^{II}(dppe)Cl_2$ to the Co^{0} species but such redox process is hindered in nonpolar *o*-dichlorobenzene.

In this study, the formation of Co^{I} species was detected by the color change of reaction mixture from the green color of $Co^{II}(dppe)Cl_2$ to red at the reduction with sodium fluorenone ketyl. After removal of unreacted sodium fluorenone ketyl by filtration, the generated $Co^{I}(dppe)_n^{+}$ (n = 1, 2) was treated with neutral fullerenes. $Co^{I}(dppe)_2Cl$ is rather strong donor and potentially it can reduce fullerenes providing the CT complexes composed of $Co^{II}(dppe)_2^{2+}$ and $C_{60}^{\bullet-}$ or $C_{70}^{\bullet-}$ radical anions. While the main product of this reaction was $\{Co(dppe)_2Cl\}(C_{60})$ (**1**), the $\{Co^{I}(dppe)_2^{+}\}(C_{60}^{\bullet-})\cdot 2C_6H_4Cl_2$ salt[12] is also crystallized in 20% yield. The $\{Co(dppe)_2Cl\}(C_{70})\cdot 0.5C_6H_4Cl_2$ (**2**) complex crystallized exclusively with C_{70}.

b). Optical properties

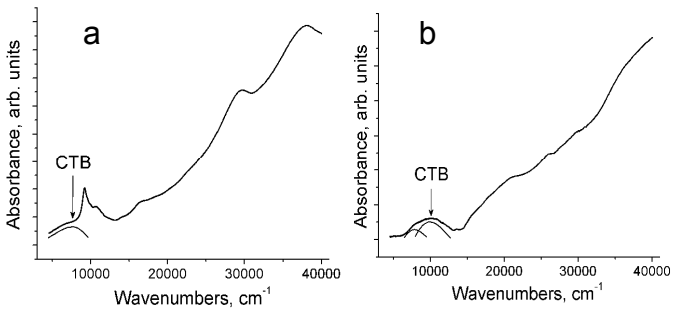

Fig. 1. Spectra of **1** (a) and **2** (b) in the UV-visible-NIR range measured at room temperature in KBr pellets prepared in anaerobic conditions.

The IR spectra of **1** and **2** are listed in Table S1 and are shown in Figs. 1S and 2S. The spectra practically seem to be the superposition of the absorption bands of $Co(dppe)_2Cl$ and fullerene anions $C_{60}^{\bullet-}$ or $C_{70}^{\bullet-}$. Neutral fullerene C_{60} shows four F_{1u} mode IR bands at 527, 576, 1183, 1429 cm^{-1} (denoted as $F_{1u}(1)$ to $F_{1u}(4)$, respectively).[5, 25, 26] While other bands exhibit only a few cm^{-1} shifts, the $F_{1u}(4)$ mode shows 37 cm^{-1} red shift when C_{60} is charged -1. The strong absorption band observed at 1393 cm^{-1} for **1** unambiguously indicates the formation of $C_{60}^{\bullet-}$. The coexistence of partially reduced or neutral C_{60} cannot be confirmed from the IR spectrum since $Co(dppe)_2Cl$ has intense absorption bands at 1433 and 530 cm^{-1} which coincide with those of neutral C_{60}. A similar situation is observed for complex **2** containing C_{70} (Table S1).

The UV-visible-NIR spectra of **1** and **2** are shown in Fig. 1. The absorption bands in the spectrum of **1** at 38000, 29700 cm^{-1} (262, 334 nm) and the weaker band at 16860 cm^{-1} (612 nm) can be attributed to C_{60} whereas the bands in the NIR range at 10650 and 9240 cm^{-1} (948, 1087 nm) (Fig. 1a) show the presence of $C_{60}^{\bullet-}$ [5,6]. The broad low-energy band of relatively weak intensity at about 7660 cm^{-1} (1300 nm) (Fig. 1a) can be ascribed to the CT transition between fullerenes or the $Co(dppe)_2Cl$ and fullerene species. Similarly, absorption bands in the spectrum of **2** at 26000 and 20840 cm^{-1} (382 and 480 nm) are ascribed to C_{70}. The broad absorption band in the NIR range can be reproduced by two Gaussian curves with maxima at about 9900 and 7500 cm^{-1} (1010 and 1330 nm, Figs. 1b and 2). The position of the latter band is close to that in the solution spectrum of monomeric $C_{70}^{\bullet-}$. [5, 6, 27] It should be noted that generally C_{70} monoanions form singly bonded $(C_{70}^{-})_2$ dimers in solids to show two bands in the NIR range at about 11360 and 8200 cm^{-1} (880 and 1220 nm, Fig. 2)[18-20]. Strong shift of the $(C_{70}^{-})_2$ band at 880 nm to 1010 nm in the spectrum of **2** proves the failure of dimer formation in **2**. So far, monomeric $C_{70}^{\bullet-}$ are preserved only in the $(Ph_4P^+)_2(C_{70}^{\bullet-})(I^-)$ salt due to the long distances between fullerenes.[28] The broad band at about 9900 cm^{-1} (1010 nm) can be attributed to CT between fullerenes or the $Co(dppe)_2Cl$ and fullerene species. Low energy CT bands

Fig. 2. The comparison of visible-NIR spectra of the $C_{70}^{\bullet-}$ radical anions in **2** (upper spectrum) and the $(C_{70}^{-})_2$ dimers in complex $(Cp_2Co^+)_2(C_{70}^{-})_2\cdot 2C_6H_4Cl_2$ (lower spectrum)[8].

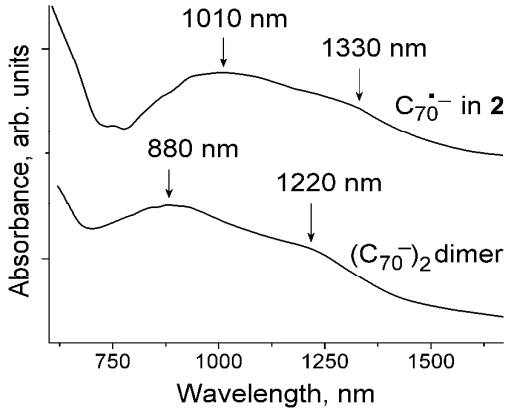

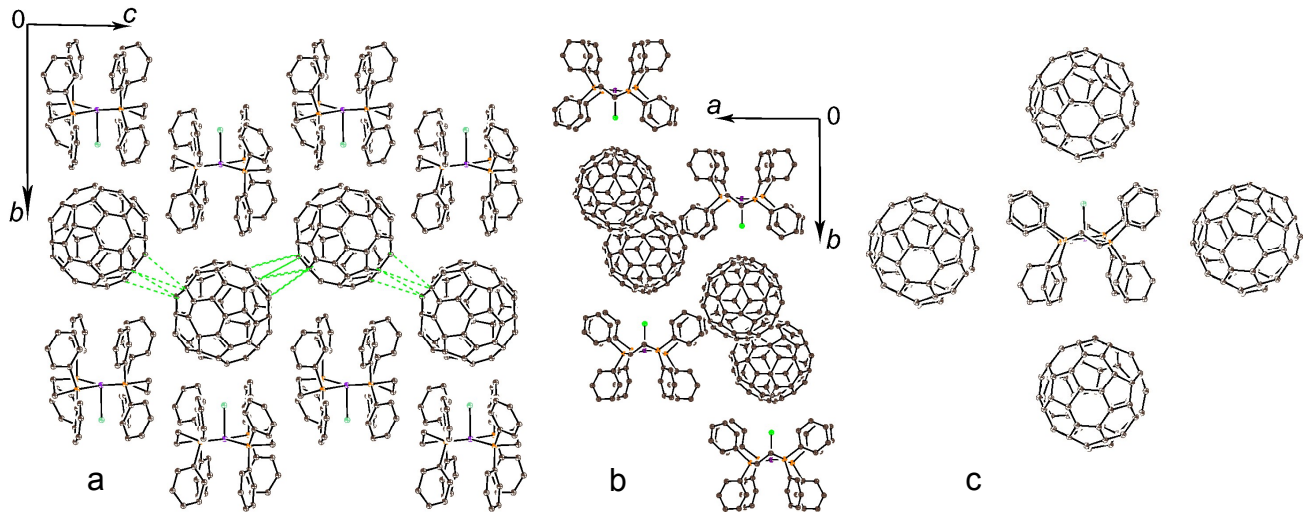

Fig. 3. (a) View on the crystal structure of **1** along the *a* axis and zigzag C_{60} chains (shortened van der Waals C···C contacts between fullerenes are shown by green dashed lines) and (b) along the *c* axis and zigzag C_{60} chains; (c) surrounding of $Co(dppe)_2Cl$ by four C_{60} cages. Only one of two C_{60} orientations is shown.

(ca. 2,000 - 5,000 cm^{-1}) which corresponds to the Drude type reflectivity spectra characteristic of metals are not observed in the spectra of both **1** and **2**.

c). Crystal structures

$\{Co(dppe)_2Cl\}(C_{60})$ (**1**) contains closely packed zigzag fullerene chains arranged along the *c* axis with equal interfullerene center-to-center (ctc) distances of 9.97 Å. This distance is noticeably shorter than the van der Waals (vdW) diameter of C_{60} (10.18 Å) and multiple vdW C···C contacts are formed between fullerenes (shown by green dashed lines in Fig. 3a). Fullerene chains are isolated (Fig. 3b), and the shortest ctc interfullerene distance between the neighboring chains is 12.53 Å.

Each $Co(dppe)_2Cl$ unit is surrounded by four C_{60} cages (Fig. 3c). Nearly spherical C_{60} is inserted into the cavities formed by four phenyl substituents of $Co(dppe)_2Cl$, and multiple vdW C,H($Co(dppe)_2Cl$)···C(C_{60}) contacts are formed. One of four surrounding fullerenes forms short Cl($Co(dppe)_2Cl$)···C(C_{60}) contacts of the 2.998-3.107 Å length. The shortest distances (5.22-5.41 Å) between cobalt and the C_{60} carbon atoms are attained with fullerene closest to the chloride anion of $Co(dppe)_2Cl$.

Fullerenes C_{70} form closely packed double chains arranged along the *a* axis in $\{Co(dppe)_2Cl\}(C_{70})\cdot 0.5C_6H_4Cl_2$ (**2**). The longer axis of C_{70} is directed along this axis, and the ctc interfullerene distance is 10.81 Å in this direction. The ctc interfullerene distance in the double chains along the *b* axis is 10.18 Å. As a result, multiple short vdW C···C contacts are formed between fullerenes (shown by green dashed lines in Fig. 4a). Double fullerene chains are completely isolated to give the ctc interfullerene distances among the neighboring double chains longer than 14 Å (Fig. 4b). Each $Co(dppe)_2Cl$ unit is

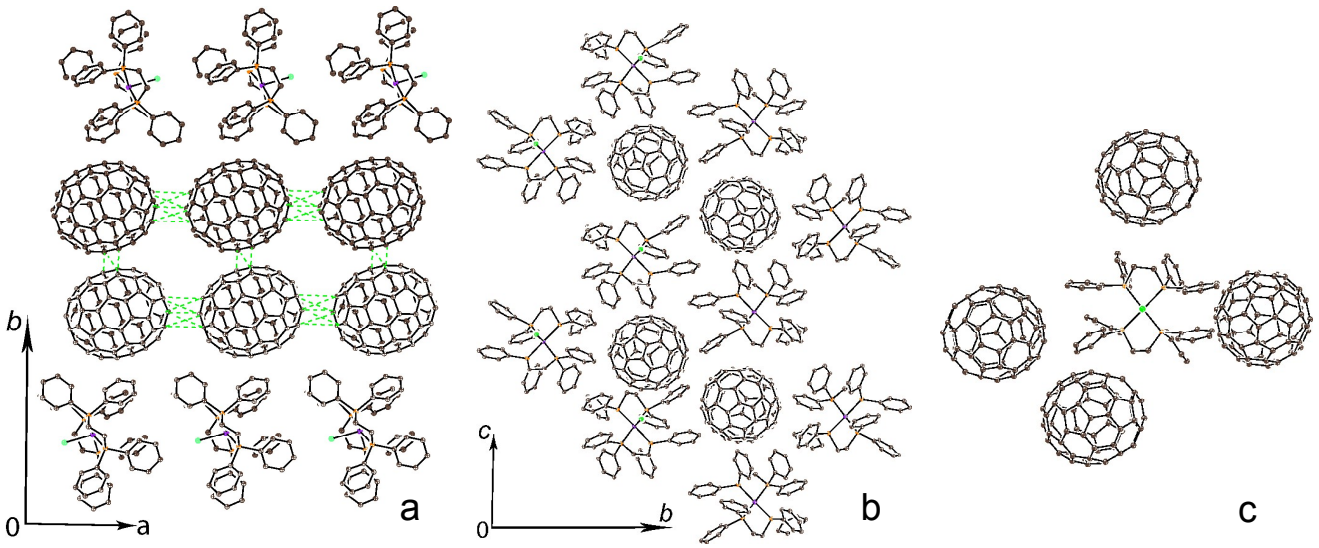

Fig. 4. (a) View on the crystal structure of **2** along the *c* axis and double C_{70} chains (shortened van der Waals C···C contacts between fullerenes are shown by green dashed lines) and (b) along the *a* axis and double C_{70} chains; (c) surrounding of $Co(dppe)_2Cl$ by four C_{70} cages. Only major fullerene orientation is shown. Solvent molecules are not shown.

surrounded by four C_{70} cages in **2** (Fig. 4c). In this case phenyl substituents cannot form suitable cavity for a larger C_{70} ellipsoid, and it is positioned asymmetrically to $Co(dppe)_2Cl$ (Fig. 4c). There are no short $Cl(Co(dppe)_2Cl)\cdots C(C_{70})$ contacts in **2** unlike the crystal structure of **1**. The shortest $Co\cdots C(C_{70})$ distances are 5.94-6.70 Å.

The arrangement of ligands around cobalt atoms in the $Co(dppe)_2Cl$ units is similar in **1** and **2.** However, these units have different bond lengths at the cobalt atoms. The cobalt atoms are located in the pyramidal environment in both units formed by four phosphorus atoms and one chloride anion. The Co atoms are not located strictly in the plane of four phosphorus atoms but move out of this plane by 0.110 and 0.124 Å towards chloride anion in **1** and **2**, respectively. The dimension of pyramidal coordination is informative to evaluate the charge on Co. As listed in Table 1, the average of Co-P length is increased according to the charge on Co (See, #0, 3-5).

Table 1. Interatomic distances (Å) in $Co(dppe)_2L$ species.

	Compound	Co-Cl	Co-P (average)	ref
#0	$\{Co^{I}(dppe)_2\}^{+}(C_{60}^{\bullet-})\cdot 2C_6H_4Cl_2$ (almost square planar)		2.193(2)	12
#1	$\{Co(dppe)_2Cl\}(C_{60})$ (**1**)	2.366(2)	2.2495(8)	this work
#2	$\{Co(dppe)_2Cl\}(C_{70})\cdot 0.5C_6H_4Cl_2$ (**2**)	2.403(3)	2.2725(8)	this work
#3	$\{Co^{II}(dppe)_2Cl\}^{+}(SnCl_3^{-})\cdot C_6H_5Cl$	2.398(2)	2.275(2)	29
#4	$\{Co^{II}(dppe)_2I\}^{+}(I^{-})\cdot CHCl_3$		2.283(3)	30
#5	$\{Co^{II}(dppe)_2(CH_3CN)\}^{2+}(BF_4^{-})_2\cdot C_3H_6O$		2.306(3)	22

The value of 2.2725(8) Å for **2** proves that Co is oxidized in this complex to almost +2, which well corresponds to the similar Co-Cl length to that of #3. Contrary, averaged Co-P length in **1** is shortened comparing to those Co^{II} materials.

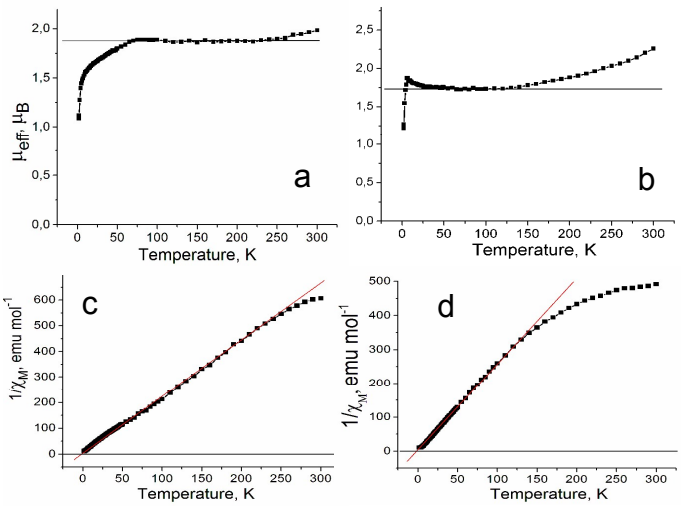

Fig. 5. Temperature dependencies for effective magnetic moments of **1** (a) and **2** (b), and reciprocal molar magnetic susceptibility of **1** (c) and **2** (d).

Comparing with that in #0, the Co in **1** is regarded not to be oxidized fully to +2. This evaluation well corresponds to the optical spectra and magnetic data for **1.**

d). Magnetic properties

Magnetic properties of **1** and **2** were studied by SQUID and EPR techniques. Effective magnetic moments of **1** and **2** are 1.98 and 2.27 μ_B at 300 K, respectively. These values are intermediate between those characteristic of the systems of one and two non-interacting S = 1/2 spins per formula unit (1.73 and 2.45 μ_B, respectively). In case of **2**, magnetic moment is closer to 2.45 μ_B than that of **1**. We suppose that paramagnetic $Co^{II}(dppe)_2Cl^{+}$ cations and $C_{60}^{\bullet-}$ or $C_{70}^{\bullet-}$ radical anions with the S = 1/2 spin state are formed in both complexes due to CT from $Co(dppe)_2Cl$ to fullerenes. Since the magnetic moment of 2.45 μ_B is expected at fully charge-transferred $\{Co^{II}(dppe)_2Cl\}^{+}(fullerene)^{\bullet-}$ state, the observed lower magnetic moments are most probably due to the coexistence of diamagnetic $\{Co^{I}(dppe)_2Cl\}^{0}(fullerene)^{0}$ with the total magnetic moments of S = 0. Moreover, magnetic moments are not constant at high temperature and increases above 220 K for **1** and 140 K for **2** (Figs. 5a and 5b). Such behavior can be explained by the increase of degree of CT from $Co(dppe)_2Cl$ and fullerenes with temperature. The low-temperature part can be approximated well by the Curie-Weiss expression with Weiss temperatures of only -2 and -3.5 K for **1** and **2**, respectively (Figs. 5c and 5d). Thus, in spite of close packing of fullerenes in **1** and **2**, only weak antiferromagnetic coupling of spins and no long range ordering are observed in both complexes. The presence of neutral diamagnetic components and disorder of fullerenes can interrupt the phase transition. Incomplete CT to fullerenes can also be the reason for the absence of fullerene dimerization in spite of their close packing in a crystal. Especially the complex **2** should be noted since the formation of stable singly bonded $(C_{70}^{-})_2$ dimers is observed in almost all the ionic compounds of C_{70} [18-20]. The similar exceptional absence of dimerization was found for C_{60} complexes with partial CT states as average.[14]

Complex **1** manifests an intense asymmetric EPR signal at room temperature which can be fitted well by three components with g_1 = 2.0968 (the linewidth (ΔH) of 15.51 mT), g_2 = 2.0488 and ΔH = 11.06 mT and g_3 = 2.0085 and ΔH = 8.16 mT (Fig. 6a). Starting Co^{I} has S = 1 or most probably S = 0 spin state. Compounds of Co^{I} with the S = 1 spin state can manifest triplet EPR signals, for example, $Co^{I}(Ph_3P)_3X$ (X = Cl, Br)[31], but these signals cannot be observed by the X-band EPR spectroscopy. Only high-frequency and -field EPRspectroscopy can be used for these purposes. Neutral fullerenes are EPR silent. Therefore, only paramagnetic $Co^{II}(dppe)_2Cl^{+}$ and the $C_{60}^{\bullet-}$ or $C_{70}^{\bullet-}$ radical anions can contribute to the EPR signals of **1** and **2**. Here, it is noted that the spin susceptibility estimated by the EPR signal intensity showed the same temperature dependency to that of magnetic susceptibility determined by SQUID technique both

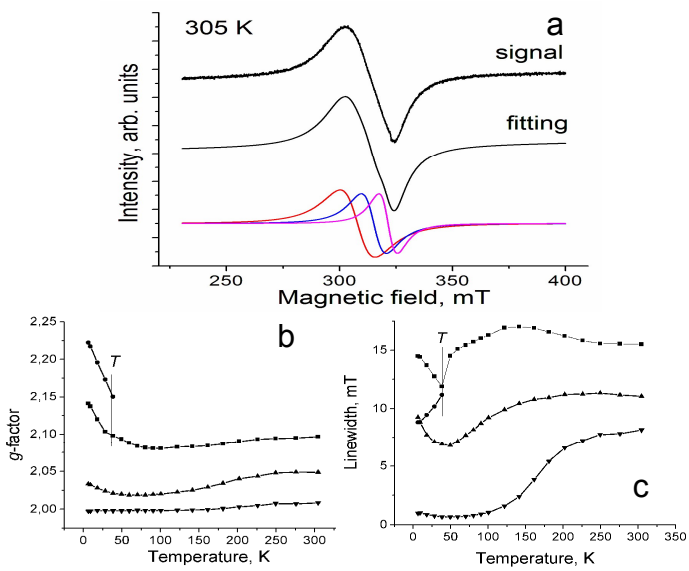

Fig. 6. (a) EPR signal for polycrystalline **1** at 305 K; temperature dependence of components of EPR signal: (b) g-factor, (c) linewidth.

for **1** and **2**. This means that there is no contribution of Co^{I} to the magnetism in these materials.

$Co^{II}(dppe)Br_2$ shows the Lorentzian EPR signal with g = 2.0357 and ΔH = 15.5 mT. However, $Co^{II}(dppe)Br_2$ has tetrahedral geometry but the $Co^{II}(dppe)_2Cl^{+}$ cations have the pyramidal environment for the cobalt atoms. Essential

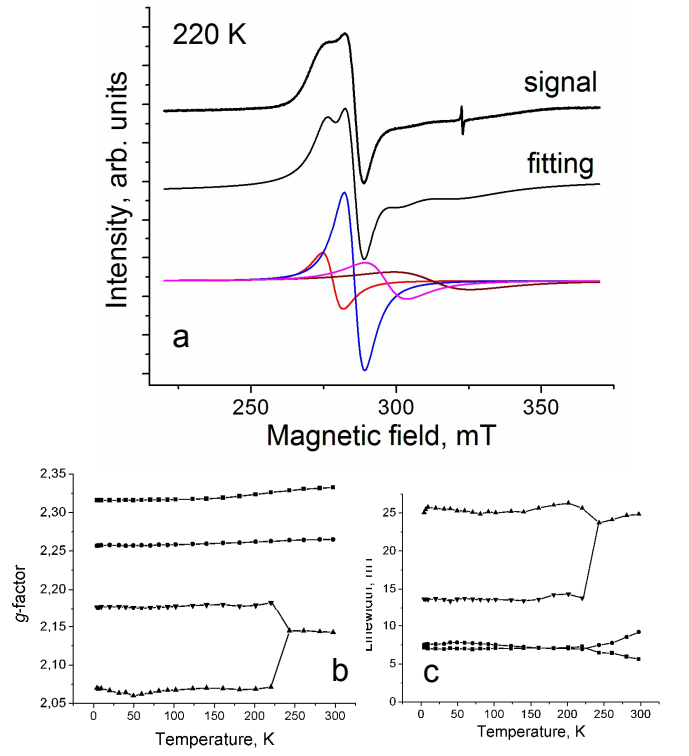

Fig. 7. EPR signal in polycrystalline **2** at 220 K (a); Temperature dependence of *g*-factor (b) and linewidth (c) of the components of EPR signal of **2**.

modification of cobalt environment at the formation of $Co^{II}(dppe)_2Cl^{+}$ can affect the EPR signal shifting *g*-factors to higher values in comparison with that of $Co^{II}(dppe)Br_2$. The signals with *g*-factor closer to that of $C_{60}^{\bullet-}$ are also observed (g_2 = 2.0488 and g_3 = 2.0085) together with the signals characteristic of Co^{II}. These signals could be ascribed to both $Co^{II}(dppe)_2Cl^{+}$ and $C_{60}^{\bullet-}$ species having exchange interaction. They are strongly narrowed with the temperature decrease (Fig. 6c) and grow in intensity with the temperature increase above 220 K. We attribute such behavior to the increase of CT degree from $Co(dppe)_2Cl$ and C_{60}. The component with g_3 = 2.0980 splits into two components below 40 K positioned at g = 2.0979 and 2.1501. Both components shift to higher *g*-factors with the temperature decrease (Fig. 6b).

Complex **2** shows an intense EPR signal at room temperature which can be fitted by three Lorentzian lines with g_1 = 2.3325 (ΔH = 5.62 mT), g_2 = 2.2649 (ΔH = 9.20 mT), and g_3 = 2.1428 (ΔH = 24.84 mT) (Fig. 7). The broad g_3-component splits into two lines below 220 K which are positioned at g = 2.1829 (ΔH = 13.86 mT) and 2.0711 (ΔH = 25.64 mT) at 220 K. It is seen that the EPR signal in **2** is broader and has essentially higher *g*-factors of the lines in comparison with those of **1**. We can suppose that lines in the EPR spectrum of **2** with lower *g*-factors of 2.18 and 2.07 have essential contribution from $C_{70}^{\bullet-}$. It is known that the $C_{70}^{\bullet-}$ radical anions in $(Ph_4P^{+})_2(C_{70}^{\bullet-})(I^{-})$ show a broad EPR signal with *g*-factor of 2.0047 (ΔH = 60 mT) at 300 K.[28] Therefore, the lines in the spectrum of **2** originating from both $Co^{II}(dppe)_2Cl^{+}$ and $C_{70}^{\bullet-}$ are essentially broader and shifted to higher *g*-factors in comparison with those of **1**. Lines with lower *g*-factors (g = 2.18 and 2.07) slightly grow in intensity with the temperature increase above 150 K and that can be also explained by the increase of CT degree from $Co(dppe)_2Cl$ to C_{70}.

Experimental

Materials

C_{60} of 99.9% purity and C_{70} of 99% purity were used from MTR Ltd. without further purification. $Co^{II}(dppe)Cl_2$ (98%) was purchased from Aldrich. Sodium fluorenone ketyl was obtained as described.[32] Solvents were purified in argon atmosphere and degassed. *o*-Dichlorobenzene ($C_6H_4Cl_2$) was distilled over CaH_2 under reduced pressure and hexane was distilled over Na/benzophenone. All manipulations for the syntheses of **1** and **2** were carried out in a MBraun 150B-G glove box with controlled argon atmosphere and the content of H_2O and O_2 less than 1 ppm. The solvents and crystals were stored in the glove box. Polycrystalline samples of **1** and **2** were placed in 2 mm quartz tubes in anaerobic conditions for EPR and SQUID measurements and sealed under 10^{-5} torr pressure. KBr pellets for IR- and UV-visible-NIR measurements were prepared in the glove box.

Synthesis

Crystals of **1** and **2** were obtained by diffusion technique. A reaction mixture was filtered into a 1.8-cm-diameter, 50 mL

glass tube with a ground glass plug, and then 30 mL of hexane was layered over the solution. Slow mixing of the solutions resulted in precipitation of crystals over 1 month. The solvent was then decanted from the crystals, and they were washed with hexane. The compositions of the obtained salts were determined from X-ray diffraction analysis on a single crystal. Due to high air sensitivity of **1** and **2**, elemental analysis could not be used to determine the composition because the salts reacted with oxygen in air before the quantitative oxidation procedure.

The crystals of $\{Co(dppe)_2Cl\}(C_{60})$ (**1**) and $\{Co(dppe)_2Cl\}(C_{70})\cdot 0.5C_6H_4Cl_2$ (**2**) were obtained by the following procedure. The reduction of green $Co^{II}(dppe)Cl_2$ (22 mg, 0.042 mmol) in 16 ml of $C_6H_4Cl_2$ with sodium fluorenone ketyl (20 mg, 0.098 mmol) during 2 hours at 100°C yielded clear red solution. The solution was cooled down to room temperature and filtered into the flask containing fullerene C_{60} (30 mg, 0.042 mmol) for preparation of **1** and fullerene C_{70} (35 mg, 0.042 mmol) for preparation of **2**. Fullerenes were dissolved in the obtained solution during 4 hours at 80°C to produce violet-red and red solutions, respectively. After cooling down to room temperatures the solutions were filtered into the tube for diffusion. The crystals of $\{Co(dppe)_2Cl\}(C_{60})$ (**1**) were obtained as black plates in 26% yield together with black elongated parallelepipeds of previously reported salt $\{Co^{I}(dppe)_2^{+}\}(C_{60}^{\bullet-})\cdot 2C_6H_4Cl_2$[12] (yield is 20%) which was identified by X-ray diffraction on several parallelepiped-shaped single crystals. The crystals of two phases had different shapes and were separated under microscope in the glove box. Purity of **1** was supported by the absence of the line at $g = 1.9986$ (ΔH = 4.57 mT) characteristic of $\{Co^{I}(dppe)_2^{+}\}(C_{60}^{\bullet-})\cdot 2C_6H_4Cl_2$. The crystals of $\{Co(dppe)_2Cl\}(C_{70})\cdot 0.5C_6H_4Cl_2$ (**2**) were obtained as black plates in the 42% yield. Testing of several crystals from the synthesis shows the presence of only one phase in this synthesis.

General

UV-visible-NIR spectra were measured in KBr pellets on a Perkin Elmer Lambda 1050 spectrometer in the 250-2500 nm range. FT-IR spectra were obtained in KBr pellets with a Perkin-Elmer Spectrum 400 spectrometer (400-7800 cm^{-1}). EPR spectra were recorded for polycrystalline samples of **1** and **2** with a JEOL JES-TE 200 X-band ESR spectrometer equipped with a JEOL ES-CT470 cryostat working between room and liquid helium temperatures. A Quantum Design MPMS-XL SQUID magnetometer was used to measure static magnetic susceptibility of **1** and **2** at 100 mT magnetic field in cooling and heating conditions in the 300 − 1.9 K range. A sample holder contribution and core temperature independent diamagnetic susceptibility (χ_d) were subtracted from the experimental values. The χ_d values were estimated by the extrapolation of the data in the high-temperature range by fitting the data with the following expression: $\chi_M = C/(T - \Theta) + \chi_d$, where C is Curie constant and Θ is Weiss temperature. Effective magnetic moment (μ_{eff}) was calculated with the formula of $\mu_{eff} = (8\cdot\chi_M\cdot T)^{1/2}$.

Crystal structure determination

The intensity data for **1** and **2** were collected on an IPDS (Stoe) diffractometer with graphite monochromated Mo-K_α radiation (λ = 0.71073 Å). The structures were solved by a direct method and refined by a full-matrix least-squares method against F^2 using SHELXL 2014/7.[33] All non-hydrogen atoms were refined anisotropically. Positions of hydrogen atoms were included into refinement in a riding model. See …….for crystallographic data in CIF format.

Crystal data of **1** at 100(2) K: $C_{112}H_{48}ClCoP_4$, M_r = 1611.76 g mol^{-1}, black plate, monoclinic, $C2/c$, a = 22.1120(6), b = 19.1090(6), c = 17.0090(4) Å, β = 107.480(2)°, V = 6855.1(3) $Å^3$, Z = 4, d_{calc} = 1.562 g cm^{-3}, μ = 0.446 mm^{-1}, $F(000)$ = 3296, $2\theta_{max}$ = 58.4°, reflections measured 36820, unique reflections 9002, reflections with $I > 2\sigma(I)$ = 6591, parameters refined 630, restraints 180, R_1 = 0.0735, wR_2 = 0.1851, G.O.F. = 1.083. The C_{60} cage is disordered over two orientations linked by a two-fold axis. CCDC 1437134.

Crystal data of **2** at 100(2) K: $C_{125}H_{50}Cl_2CoP_4$, M_r = 1805.36 g mol^{-1}, black plate, monoclinic, $P2_1/n$, a = 10.8104(3), b = 39.8917(10), c = 18.2142(5) Å, β = 100.133(2)°, V = 7732.3(4) $Å^3$, Z = 4, d_{calc} = 1.551 g cm^{-3}, μ = 0.438 mm^{-1}, $F(000)$ = 3684, max. $2\theta_{max}$ = 53.5°, reflections measured 47143, unique reflections 15869, reflections with $I > 2\sigma(I)$ = 10991, parameters refined 821, restraints 24, R_1 = 0.0814, wR_2 = 0.2035, G.O.F. = 1.000. The C_{70} cage is disordered between three orientations with the 0.45/0.30/0.25 occupancies. The solvent $C_6H_4Cl_2$ molecule is statistically disordered between two orientations. CCDC 1437135.

Conclusions

The interaction of the Co^{I} species generated by the reduction of $Co^{II}dppeCl_2$ allows the preparation of CT complexes $\{Co(dppe)_2Cl\}(C_{60})$ (**1**) and $\{Co(dppe)_2Cl\}(C_{70})\cdot 0.5C_6H_4Cl_2$ (**2**). Both complexes contain the $C_{60}^{\bullet-}$ or $C_{70}^{\bullet-}$ radical anions and the $Co^{II}(dppe)_2Cl^+$ cations formed as a result of CT from $Co^{I}(dppe)_2Cl$ to fullerenes. CT becomes possible due to strong donor property of $Co^{I}(dppe)_2Cl$ which is enough to produce fullerene$^{\bullet-}$ radical anions. However, most probably CT is not complete and diamagnetic $\{Co^{I}(dppe)_2Cl\}^0$ and neutral fullerenes are also preserved in the samples. As a result, in spite of close packing of fullerenes in the chains only weak magnetic coupling of spins is observed and fullerenes are not dimerized in both complexes. The absence of dimerization allows for the first time to observe solid state optical spectrum of monomeric $C_{70}^{\bullet-}$ radical anions and to determine their molecular structure. It is seen also that, organometallic compounds with strong donor properties can be promising components to design fullerene complexes with partial CT.

Acknowledgements

The work was supported by Russian Science Foundation (project no. 14-13-00028) and by JSPS KAKENHI Grant Numbers 23225005 and 26288035.

Notes and references

[a]Institute of Problems of Chemical Physics RAS, Chernogolovka, Moscow region, 142432 Russia;
[b]Chemistry Department, Moscow State University, Leninskie Gory,119991 Moscow, Russia;
[c]Research Center for Low Temperature and Materials Sciences, Kyoto University, Sakyo-ku, Kyoto 606-8501, Japan;
[d]Faculty of Agriculture, Meijo University, 1-501 Shiogamaguchi, Tempaku-ku, Nagoya 468-8502, Japan;
[e]Toyota Physical and Chemical Research Institute, 41-1, Yokomichi, Nagakute, Aichi 480-1192, Japan.

Electronic Supplementary Information (ESI) available: IR spectra of **1** and **2**. This material is available free of charge via Internet at …..

1 K. Tanigaki and K. Prassides, *J. Mater. Chem.* 1995, **5**, 1515.
2 P. W. Stephens, G. Bortel, G. Faigel, M. Tegze, A. Jánossy, S. Pekker, G. Oszlanyi and L. Forró. *Nature,* 1994, **370**, 636.
3 D. V. Konarev, S. S. Khasanov, A. Otsuka, M. Maesato, G. Saito and R. N. Lyubovskaya, *Angew. Chem. Int. Ed.* 2010, **49**, 4829.
4 P.W. Stephens, D. Cox, J.W. Lauher, L. Mihaly, J.B. Wiley, P.-M. Allemand, A. Hirsch, K. Holczer, Q. Li, J.D. Thompson and F. Wudl, *Nature* 1992, **355**, 331.
5 D.V. Konarev and R.N. Lyubovskaya, *Russ. Chem. Rev*., 2012, **81**, 336.
6 C. A. Reed and R. D. Bolskar, *Chem. Rev*. 2000, **100**, 1075.
7 W.C. Wan, X. Liu, G.M. Sweeney, W.E. Broderick, *J. Am. Chem. Soc.,* 1995, **117**, 9580.
8 D. V. Konarev, S. S. Khasanov, G. Saito, A. Otsuka, Y. Yoshida, R. N. Lyubovskaya*, J. Am. Chem. Soc.*, 2003, **125**, 10074.
9 D. V. Konarev, S. S. Khasanov, I. I. Vorontsov, G. Saito, Yu. M. Antipin and R.N. Lyubovskaya, *Inorg. Chem*., 2003, **42**, 3706.
10 C. Bossard, S. Rigaut, D. Astruc, M. -H. Delville, G. Félix, A. Février-Bouvier, J. Amiell, S. Flandrois and P. Delhaès. *J. Chem. Soc., Chem. Commun*., **1993**, 333.
11 D. V. Konarev, S. S. Khasanov, A. Otsuka, H. Yamochi, G. Saito, R. N. Lyubovskaya, *Inorg. Chem*., 2014, **53**, 6850.
12 D. V. Konarev, A. V. Kuz`min, S. V. Simonov, S. S. Khasanov, E. I. Yudanova and R.N. Lyubovskaya, *Dalton Trans*, 2011, **40**, 4453.
13 M. Schulz-Dobrick and M. Jansen, *Angew. Chem., Int. Ed*., 2008, **47**, 2256.
14 D. V. Konarev, S. S. Khasanov, M. Ishikawa, E. I. Yudanova, A. F. Shevchun, M. S. Mikhailov, P. A. Stuzhin, A. Otsuka, H. Yamochi, G. Saito and R.N. Lyubovskaya, *Chem*istry Select, 2016, in press. DOI: 10.1002/slct.201500021.
15 D. V. Konarev, S. S. Khasanov, S. I. Troyanov, Y. Nakano, K. A. Ustimenko, A. Otsuka, H. Yamochi, G. Saito and R. N.Lyubovskaya, *Inorg. Chem*., 2013, **52**, 13934.
16 D. V. Konarev, S. I. Troyanov, Y. Nakano, K. A. Ustimenko, A. Otsuka, H. Yamochi, G. Saito and R. N. Lyubovskaya, *Organomet.*, 2013, **32**, 4038.
17 D. V. Konarev, S. I. Troyanov, K. A. Ustimenko, Y. Nakano, A. F. Shestakov, A. Otsuka, H. Yamochi, G. Saito and R.N. Lyubovskaya, *Inorg. Chem.,* 2015, **54**, 4597.
18 D. V. Konarev, S. S. Khasanov, I. I. Vorontsov, G. Saito, Yu. A. Antipin, A. Otsuka and R. N. Lyubovskaya, *Chem. Commun*., 2002, 2548.
19 D. V. Konarev, S. S. Khasanov, S. V. Simonov E. I. Yudanova and R. N. Lyubovskaya, *CrystEngComm*., 2010, **12**, 3542.
20 D. V. Konarev, A. V. Kuzmin, S. V. Simonov, S. S. Khasanov, A. Otsuka, H. Yamochi, G. Saito and R.N. Lyubovskaya*, Dalton Trans*., 2012, **41**, 13841.
21 D. Dubois, K. M. Kadish, S. Flanagan, R. F. Haufler, L. P. F. Chibante and L. J. Wilson. *J. Am. Chem. Soc.,* 1991, **113**, 4364.
22 R. Ciancanelli, B. C. Noll, D. L. DuBois and M.R. DuBios, *J. Am. Chem. Soc.,* 2002, **124**, 2984.
23 K. Kuwata and D. H. Geske, *J. Am. Chem. Soc.*, 1964, **86**, 2101.
24 R. O. Loutfyc, K. Hsiaob, S. Ong and B. Keoshkeria, *Can. J. Chem*. 1984, **62**, 1877.
25 T. Picher, R. Winkler and H. Kuzmany, *Phys. Rev. B*, 1994, **49**, 15879.
26 V. N. Semkin, N. G. Spitsina, S. Krol and A. Graja, *Chem. Phys. Lett*. 1996, **256**, 616.
27 D. V. Konarev, N. V. Drichko and A. Graja, *J. Chim. Phys.*, 1998, **95**, 2143.
28 A. Penicaud, A. P. Perez-Benitez, R. Escudero and C. Coulon, *Solid State Commun.,* 1995, **96**, 147.
29 J. K. Stalick, P. W. R. Corfield and D. W. Meek, *Inorg. Chem*., 1973, **12**, 1668.
30 S. Aizawa, K. Fukumoto and T. Kawamoto, *Polyhedron*, 2013, **62**, 37.
31 J. Krzystek, A. Ozarowski, S. A. Zvyagin and J. Telser, *Inorg. Chem.*, 2012, **51**, 4954.
32 D. V. Konarev, S. S. Khasanov, E. I. Yudanova, R. N. Lyubovskaya, *Eur. J. Inorg. Chem.,* 2011, 816.
33. G. M. Sheldrick, *Acta Crystallogr., Sect. A: Fundam. Crystallogr.* 2008, **64**, 112.